Switching properties of a tunneling junction connected to a spin valve

P. Weinberger

Center for Computational Nanoscience, Seilerstätte 10/22, A1010 Vienna, Austria and Department of Physics, New York University, 4 Washington Place, New York, New York 10003, USA

(Received 5 January 2011; revised manuscript received 3 February 2011; published 12 April 2011)

The switching properties of a prototype system containing a spin valve as well as a tunneling junction are investigated by means of a spin-polarized fully relativistic approach. Shown are the changes in the free energy and in the magnetoresistance when the orientation of the magnetization in the magnetic slabs of such a system is changed individually. It is demonstrated that the existence of a stable and a metastable state, a necessary condition for a switching device, is essentially determined by the free energy contributions of the interfaces of that magnetic slab that is part of the spin valve as well as of the tunneling junction. Furthermore, in estimating individual switching times, it is found that most of the gain in magnetoresistance occurs within a time range of about 20 ps, the time to achieve complete switching, however, being about 1.5 ns, which is close to what is found in recent experimental results.

DOI: 10.1103/PhysRevB.83.134413 PACS number(s): 75.70.−i, 75.47.−m, 75.75.−c

I. INTRODUCTION

In the past there seemed to be a strict separation between spin valves and tunneling junctions, or, to speak loosely, between giant magnetoresistance and tunneling magnetoresistance; see, e.g., Refs. 1–12. Lately, however, systems have been investigated experimentally[13–16] as well as theoretically[17–19] that contain a spin-valve-type part and a tunneling part, since it turned out that a combination of both might be (is) of considerable technological interest. Furthermore, nowadays no longer is only the size of the change in magnetoresistance when applying an external magnetic field or a current important, but also the switching time.[16,20–22] While the design of suitable systems consisting of a spin valve and a tunneling junction is a materials science problem and therefore falls into the realm of industrial research, the question of the switching time can only be solved using time-resolvable instrumentations. In particular, the use of pulsed electric fields and of suitable time-resolved means to record the response has led already to quite an accurate characterization of the temporal aspects of switching.

From a theoretical standpoint of view of course both of these new developments are challenging, in particular, if a microscopic description and interpretation is to be given. To characterize the switching of a spin valve plus tunneling junction (SV-TJ) system on an *ab initio* level not only implies (a) investigation of the various interface effects and monitoring of changes caused by changes in the orientation of the magnetization and (b) evaluation of the corresponding electric transport properties, but also (c) estimation of the time needed to achieve complete switching.

II. COMBINED SPIN VALVES AND TUNNELING JUNCTIONS

A typical SV-TJ system (see Fig. 1) consists of three magnetic slabs, the one in the middle being part of the spin valve as well as of the tunneling junction. Suppose that in each of these magnetic slabs the orientation of the magnetization assumes a particular (uniform) direction. If **x** and **y** denote the in-plane coordinates and **z** the orthogonal complement (surface normal) then these directions can in principle be characterized by three pairs of angles (Θ_i, Φ_i), $i = 1,2,3$, where Θ_i refers to a (clockwise) rotation around the in-plane y axis and Φ_i to such a rotation around the z axis. For example, keeping Φ_i fixed to 0, by varying Θ_i from 0 to 90°, the orientation of the magnetization in the ith magnetic slab changes in the xz plane from **z** to **x**, i.e., from out of plane to in plane.

Since experimentally studied magnetic tunneling junctions with a spin-valve part very often consist of a rather complicated sequence of functional layers, sometimes of unspecified thickness, mostly prepared by combining e-beam and optical lithography, in the following a model system is chosen [see (1)], in which the tunneling barrier is represented by a vacuum barrier of width of about 10 Å, i.e., a barrier that indeed guarantees tunneling between the two magnetic slabs forming the tunneling junction. The magnetic slabs are Co connected to a Cu lead, and $Co_{90}Fe_{10}$, one of them being connected to a Permalloy lead ($Ni_{80}Fe_{20}$) which in turn serves also as a soft magnet. As the center of the vacuum barrier contains nearly no electric charge, this system can be viewed as a stack of two subsystems, whose electronic structures can be evaluated separately as free surfaces.[23] Here it is assumed that the Fermi energy of subsystem 1 [see (1)] applies throughout the whole system. It should be noted that considered as bulk materials the lattice mismatch between fcc Cu and fcc $Ni_{80}Fe_{20}$ is less than 2%. All calculations were performed using the spin-polarized relativistic screened Korringa-Kohn-Rostoker method[24,25] and by means of the fully relativistic Kubo equation,[24,25] applying the same numerical setup as described in Ref. 17.

$$\underbrace{\mathrm{Ni_{80}Fe_{20}(111)/\overbrace{(Co_{90}Fe_{10})_5}^{(\Theta_1,\Phi_1)}/Cu_n/\overbrace{(Co_{90}Fe_{10})_5}^{(\Theta_2,\Phi_2)}/Vac_2}\cdots}_{\text{subsystem 1}}$$
$$\cdots\,\mathrm{Vac}\underbrace{\overbrace{\mathrm{Vac_2/Co_2}}^{(\Theta_3,\Phi_3)}/\mathrm{Cu(111)}}_{\text{subsystem 2}}. \qquad (1)$$

In the following first one particular case, namely, $n = 7$ in (1), is considered in full detail, and only then will n be varied.

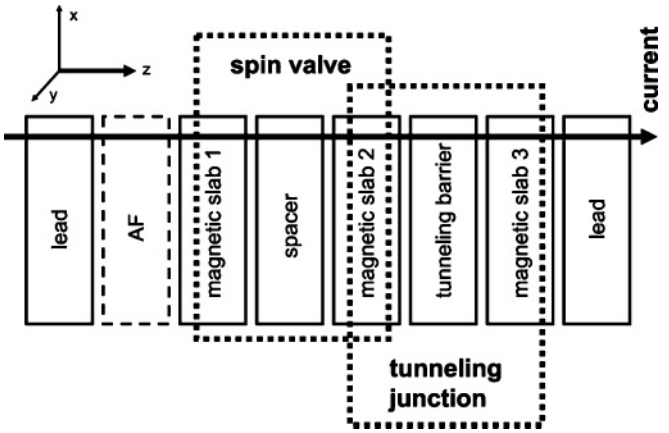

FIG. 1. Schematic view of a tunneling junction connected to a spin valve: **x** and **y** are the in-plane coordinate axes; **z** is parallel to the surface normal. In realistic samples AF usually denotes a synthetic antiferromagnet. Here the left lead and the AF part are replaced by a semi-infinite Permalloy lead with the orientation of the magnetization pointing uniformly along the surface normal (**z**).

A. Free energy

In principle, apart from the direction of the magnetization in the $Ni_{80}Fe_{20}$ lead, which was chosen to point along the surface normal, the free energy in this system forms a hypersurface with respect to the six angles specifying the orientations of the magnetization in the three magnetic slabs,

$$\Delta E\,(\mathcal{C},\mathcal{C}_0;n) = E(\mathcal{C};n) - E(\mathcal{C}_0;n) \tag{2}$$
$$= \sum_{i=1,n} \Delta E_i\,(\mathcal{C},\mathcal{C}_0;n) = \sum_{i=1,n} E_i(\mathcal{C};n) - E_i(\mathcal{C}_0;n),$$

$$\mathcal{C} = \{(\Theta_1,\Phi_1)\,;(\Theta_2,\Phi_2);(\Theta_3,\Phi_3)\}\,, \tag{3}$$
$$\mathcal{C}_0 = \{(\Theta_1,\Phi_1)^{(r)}\,;(\Theta_2,\Phi_2)^{(r)};(\Theta_3,\Phi_3)^{(r)}\},$$

where $\mathcal{C}_0$ corresponds to a suitable reference configuration and the $\Delta E_i\,(\mathcal{C},\mathcal{C}_0;n)$ are the so-called layer-resolved free energies.[24,25] The orientation of the magnetization in the leads is chosen to point along the surface normal.

Let (**x**,**y**,**z**) be a shorthand notation for the case that in the first magnetic slab the orientation of the magnetization points along **x**, ($\Theta_1 = 90°, \Phi_1 = 0$), in the second along **y**, ($\Theta_2 = 90°, \Phi_2 = 90°$), and in the third along **z**, ($\Theta_3 = 0, \Phi_3 = 0$). Since the magnetic slab in the center of the system is part of a spin valve as well as of a tunneling junction, in particular the switching properties of this slab are of quite some interest not only in experimental (technological) studies but also from a theoretical point of view. Fortunately the orientation of the magnetization in the left $Co_{90}Fe_{10}$ slab [see (1)] is tightly bound to that in the left lead. As shown in Fig. 2, even small deviations from the surface normal give rise to substantial anisotropy effects caused by the $Ni_{80}Fe_{20}/Co_{90}Fe_{10}$ interface, implying that only the orientations of the magnetization in the magnetic slabs forming the tunneling junction have to be varied, i.e., in Eq. (2) Θ_1, Φ_1 can be set to zero.

By using (**z**,**z**,**x**) as reference configuration in Eq. (2) the corresponding free energy is calculated and shown in the top part of Fig. 3 as the orientation of the magnetization changes continuously within the xz plane to (**z**,**z**,**z**), and from there

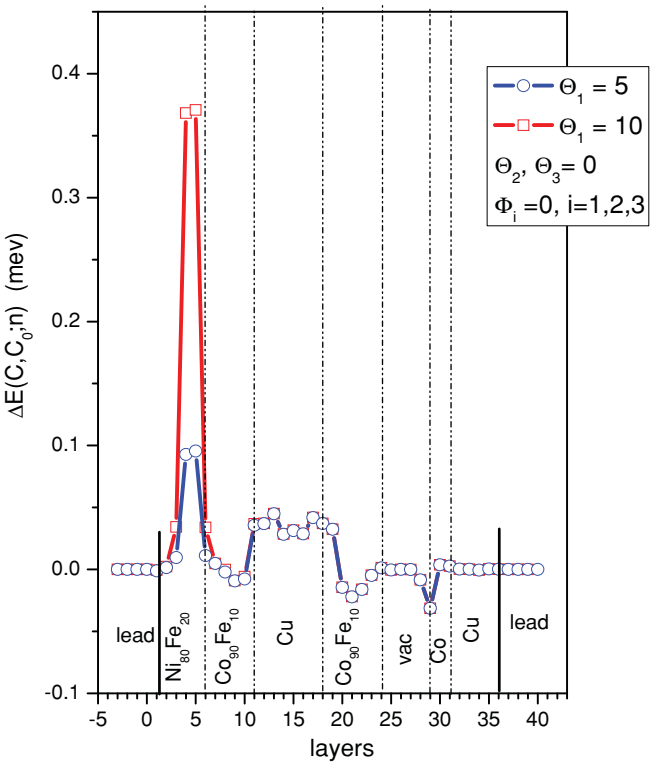

FIG. 2. (Color online) Layer-resolved free energies $\Delta E_i(C,C_0;n)$. $C = ((\Theta_1,0);(0,0),(0,0))$, $\Theta_1 = 5,10$, $n = 7$, i.e., the orientation in the first CoFe slab is slightly moved out of a direction along the surface normal. The reference configuration is (**z**,**z**,**z**).

to (**z**, − **z**,**z**). For the presentation in this figure a "running" angle Θ is used, the individual regimes of the rotations being separated by vertical lines. Note that by definition, at $\Theta = 90°$, 180°, and 270°, the slope of $\Delta E\,(\mathcal{C},\mathcal{C}_0)$ with respect to $\Delta\Theta$ is zero. In Fig. 4 (**z**,**z**,**z**) serves as reference configuration $\mathcal{C}_0$. Depicted there are the layer-resolved energies when $\mathcal{C}$ = (**z**,**z**,**x**) (top), (**z**,**x**,**z**) (middle), and (**z**,−**z**,**z**)(bottom). As can be seen in all three cases the contribution from the Co slab to the free energy is negative, i.e., the Co slab prefers to be oriented in plane. Actually, the top figure "only" reproduces the well-known fact that two monolayers (ML) of Co on Cu(111) are oriented in plane. Exactly for this reason in Fig. 3 (**z**,**z**,**x**) is chosen as reference configuration, namely, the one with the lowest energy.

Returning to the top entry in Fig. 3, one can see that (**z**,**z**,**x**) is separated from (**z**, − **z**,**z**) by a maximum of the anisotropy energy at (**z**,**z**,**z**) such that (**z**, − **z**,**z**) is a metastable state. From the middle entry in Fig. 4 it is evident that this maximum in the anisotropy energy at (**z**,**z**,**z**) is caused by the interfaces of the center magnetic slab with the tunneling part of the system and partially also with the spin-valve part, augmented by some contributions from the spacer. The anisotropy energy at (**z**, − **z**,**z**), on the other hand (see the bottom entry of Fig. 4) is mainly due to contributions from the spacer. This alone is already an interesting finding since the actual value of the anisotropy energy at (**z**,**x**,**z**) can be modified by the choice of the nonmetallic slab causing tunneling.

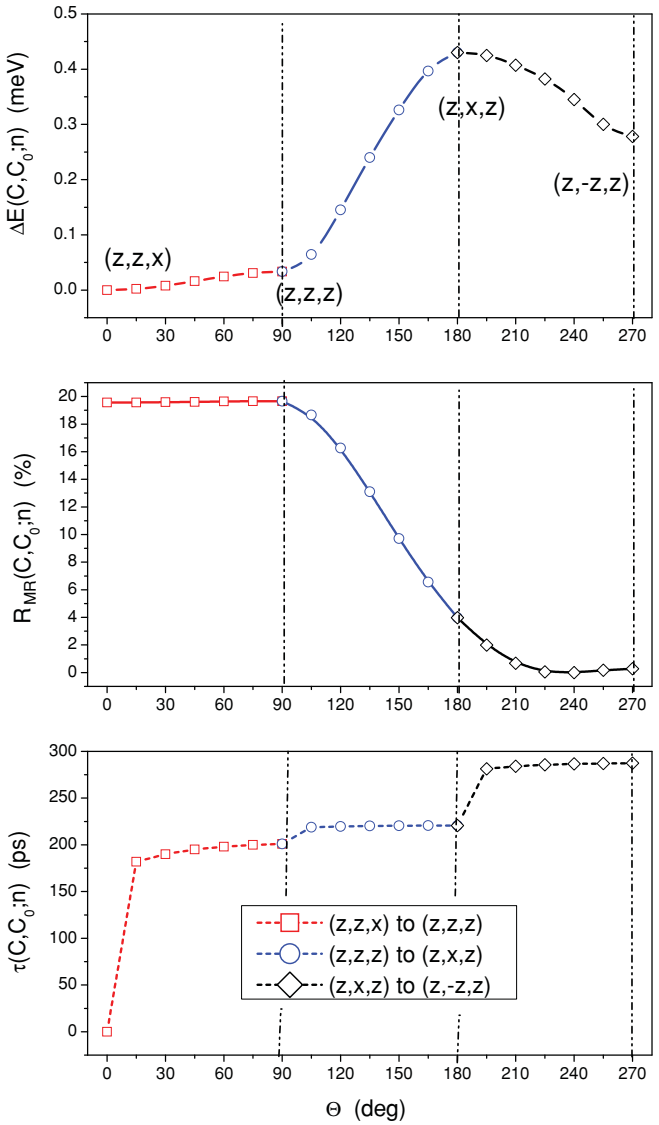

FIG. 3. (Color online) Free energy corresponding to rotations of the orientation of the magnetization in the third magnetic slab, $0 \leqslant \Theta \leqslant 90^\circ$, and the magnetic slab in the middle of the system, $90^\circ \leqslant \Theta \leqslant 270^\circ$. Special magnetic configurations are marked explicitly.

B. Magnetoresistance

In a similar manner as in Eq. (2) the difference in the zz-like resistivity $\Delta\rho_{zz}(\mathcal{C},\mathcal{C}_0)$ between two configurations can be defined and the corresponding magnetoresistance ratio (MR), $R_{\rm MR}(\mathcal{C},\mathcal{C}_0;n)$,

$$\Delta\rho_{zz}(\mathcal{C},\mathcal{C}_0;n) = \rho_{zz}(\mathcal{C};n) - \rho_{zz}(\mathcal{C}_0;n), \tag{4}$$

$$R_{\rm MR}(\mathcal{C},\mathcal{C}_0;n) = \Delta\rho_{zz}(\mathcal{C},\mathcal{C}_0;n)/\rho_{zz}(\mathcal{C};n). \tag{5}$$

As can be seen from Fig. 3, by changing the configuration from $(\mathbf{z},\mathbf{z},\mathbf{x})$ to $(\mathbf{z},-\mathbf{z},\mathbf{z})$ the magnetoresistance changes by about 20%. It is interesting to note that because from $(\mathbf{z},\mathbf{z},\mathbf{x})$ to $(\mathbf{z},\mathbf{z},\mathbf{z})$ and then from $(\mathbf{z},\mathbf{x},\mathbf{z})$ to $(\mathbf{z},-\mathbf{z},\mathbf{z})$ the MR changes very little, the MR seems to be determined by a change of orientation in the center magnetic layer only: the local maximum in $\Delta E(\mathcal{C},\mathcal{C}_0)$ at $(\mathbf{z},\mathbf{x},\mathbf{z})$ is not reflected as such in the magnetoresistance.

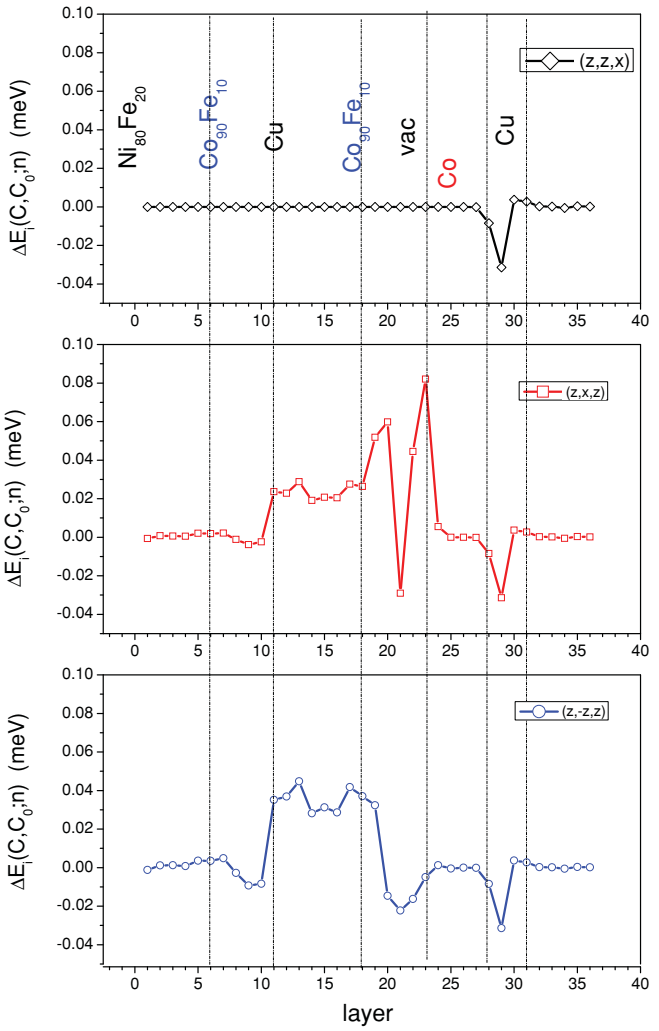

FIG. 4. (Color online) Layer-resolved free energies $\Delta E_i(C,C_0;n)$. For all three entries the reference configuration is $(\mathbf{z},\mathbf{z},\mathbf{z})$. The top entry refers to rotations from $C_0 = (\mathbf{z},\mathbf{z},\mathbf{z})$ to $C = (\mathbf{z},\mathbf{x},\mathbf{z})$, the middle one to $C = (\mathbf{z},\mathbf{x},\mathbf{z})$, the bottom one to $C = (\mathbf{z},-\mathbf{z},\mathbf{x})$.

C. Switching times

Since the derivative of the free energy $\Delta E(C,C_0;n)$ with respect to the orientation of the magnetization is nothing but the internal field $\vec{H}^{\rm eff}(C,C_0;n)$ in the Landau-Lifshitz-Gilbert equation, the so-called relaxation term in that equation,

$$\frac{d\vec{n}(C,C_0,t;n)}{dt} = \alpha\vec{n}(C,C_0,t) \times [\vec{n}(C,C_0,t)\vec{H}^{\rm eff}(C,C_0;n)], \tag{6}$$

$$\vec{n}(C,C_0,t;n) = \vec{m}(C,C_0,t;n)/m_0(n), \tag{7}$$

$$m_0(n) = L^{-1}\sum_{i=1,L} m_i(n), \tag{8}$$

can be used to estimate the time $\tau(C,C_0;n)$ needed to move from configuration C_0 to configuration C. In Eq. (7) $m_0(n)$ is an average over those layers in which the orientation of the magnetization is rotated; see, e.g., Ref. 17. By using a Gilbert damping constant of $\alpha = 1$, in the bottom part of Fig. 3 the switching time is displayed versus the running angle Θ. It should be noted that in Eq. (6) both $m_0(n)$ and $\vec{H}^{\rm eff}(C,C_0)$, refer to *ab initio* data obtained on a fully

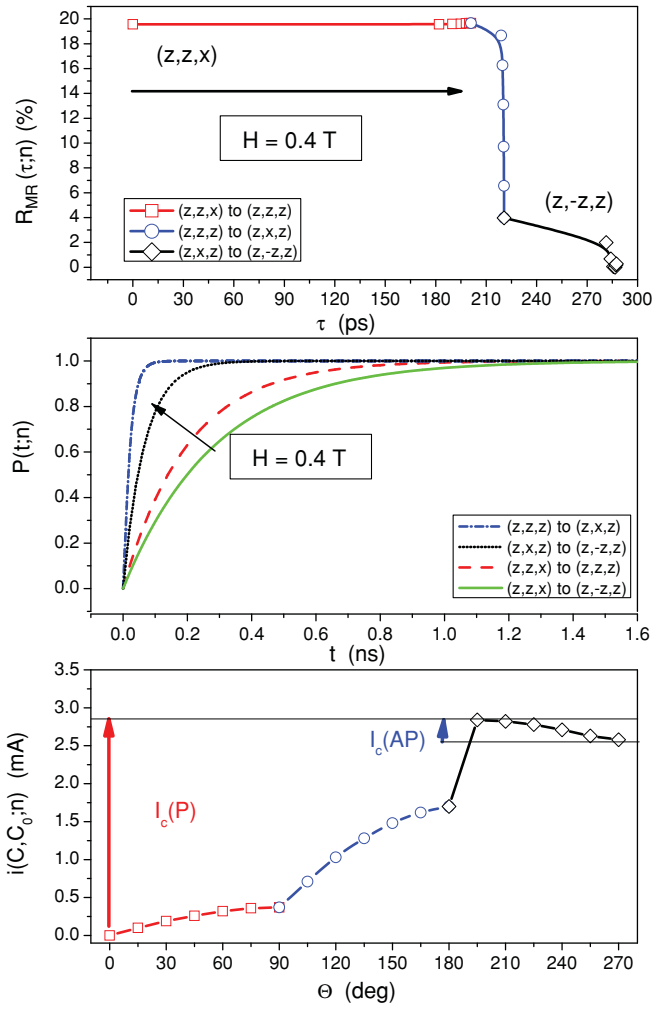

FIG. 5. (Color online) Magnetoresistance (top) and switching probability (middle) versus the switching time. Bottom: current versus rotation angle. $0 \leqslant \Theta \leqslant 90^\circ$ refers to the Co slab and $90^\circ \leqslant \Theta \leqslant 270^\circ$ to the magnetic slab in the middle of the system. Special magnetic configurations are marked explicitly. Also indicated is the effect of applying a small external magnetic field to switch the Co slab from in plane to perpendicular.

relativistic level. The only adjustable parameter is therefore α.[26] Use of a value of $\alpha < 1$ gives the corresponding switching time $\tau_{\alpha<1}(C,C_0;n) = \alpha^{-1}\tau_{\alpha=1}(C,C_0;n)$; see Ref. 27.

In order to understand Fig. 3 properly one has to recall that (a) most of an individual switching time is used up in leaving a configuration with zero derivative in $\Delta E(C,C_0;n)$, and (b) the switching times are additive. If $\tau_1(n)$ denotes the time needed to reorient from $(\mathbf{z},\mathbf{z},\mathbf{x})$ to $(\mathbf{z},\mathbf{z},\mathbf{z})$ and $\tau_2(n)$ that from $(\mathbf{z},\mathbf{z},\mathbf{z})$ to $(\mathbf{z},\mathbf{x},\mathbf{z})$ then the switching time from $(\mathbf{z},\mathbf{z},\mathbf{x})$ to $(\mathbf{z},\mathbf{x},\mathbf{z})$ is $\tau_1(n) + \tau_2(n)$. As can be guessed from the top part of Fig. 3, most of the total switching time $\tau(n) = \tau_1(n) + \tau_2(n) + \tau_3(n)$ is needed for the reorientation of the Co slab, which is the slow process.

In the top part of Fig. 5 $R_{\mathrm{MR}}(C,C_0;n)$ is displayed as an implicit function of the switching times $\tau(C,C_0;n)$ along these three paths. As can be seen the major drop in the magnetoresistance occurs within about 20 ps.

D. Switching probabilities

Suppose a simple first-order rate differential equation can be used for the switching of the orientation of the magnetization in a spin valve,[28] then the following probability function for the switching can be assumed:

$$P_k(t;n) = 1 - \exp[-t/\tau_k(n)] \tag{9}$$

with $\tau_k(n)$ being as before the switching time along a particular path. In the middle part of Fig. 5 the switching probabilities are displayed for the individual processes and for the total switching time $\tau_0(n)$. Obviously complete switching from $(\mathbf{z},\mathbf{z},\mathbf{x})$ to $(\mathbf{z},-\mathbf{z},\mathbf{x})$ takes about 1.5 ns, although some of the individual processes are much faster.

E. Critical currents

Although the studied system only serves as an academic example, the critical currents needed to achieve switching might be of interest. Assuming a particular cross section A_0 (in the present case 100×100 nm^2), an approximate relation

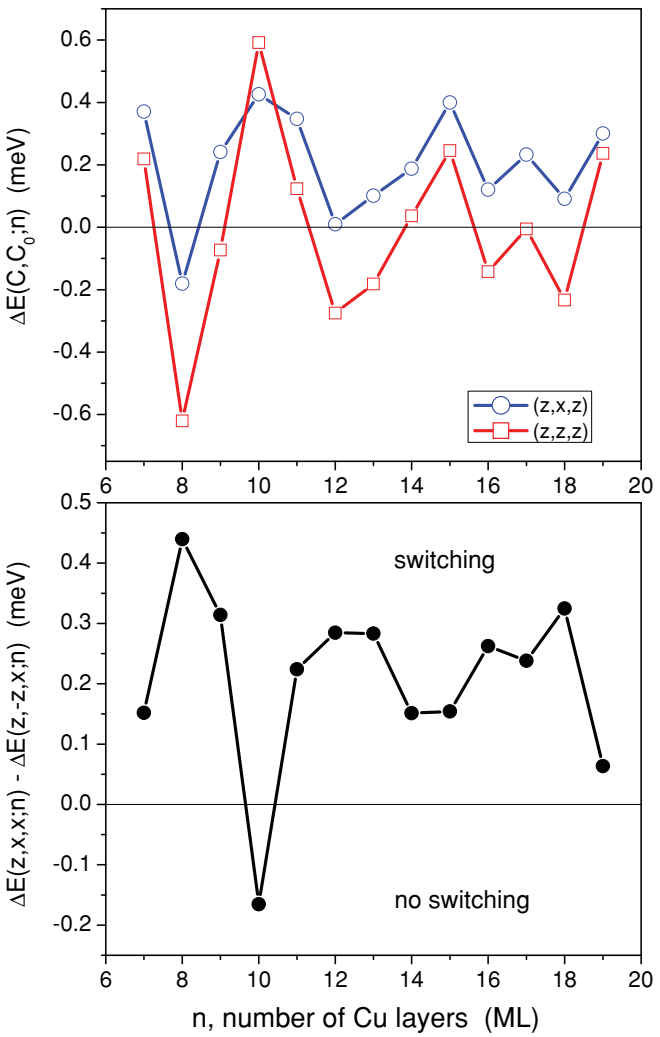

FIG. 6. (Color online) Free energy $\Delta E(C,C_0;n)$ (top) and difference in free energies between the $(\mathbf{z},\mathbf{x},\mathbf{x})$ and $(\mathbf{z},-\mathbf{z},\mathbf{x})$ configurations (bottom) versus the number of Cu spacer layers.

for the current can be given as discussed in detail in Ref. 27:

$$i(C,C_0;n) = \sqrt{\frac{A_0}{\tau(C,C_0;n)}}\sqrt{\frac{\Delta E(C,C_0;n)}{nd_\perp \rho_{zz}(C;n)}}. \qquad (10)$$

The critical current is then defined as the current that has to be applied in order to reach the maximum in the free energy; see Fig. 3. As can be seen from the bottom entry of Fig. 5 about 2.7 mA are needed to switch the system from $(\mathbf{z},\mathbf{z},\mathbf{x})$ to $(\mathbf{z},-\mathbf{z},\mathbf{x})$. It should be noted that in Eq. (10) $nd_\perp\rho_{zz}(C;n)$ refers to the so-called sheet resistance, $d_\perp$ being the interplane spacing. Clearly enough, for a given value of A_0 because of $\tau(C,C_0;n)$ the value of $i(C,C_0;n)$ does depend on the choice for the Gilbert damping parameter.

Also indicated in Fig. 5 is the effect of an external magnetic field that can be used to reorient the magnetization in the Co slab to be perpendicular to the planes of the atoms (before applying a current). For two Co layers on a Cu(111) lead this field is about 0.4 T. Obviously, to achieve complete switching $P_k(t;n) = 1$, use of such an external field in addition to a current driving the switching process can reduce the necessary time t by almost one order of magnitude.

III. DISCUSSION

Since now one particular case, namely, for $n = 7$, has been discussed in detail, the remaining question is what changes are to be expected when the number of spacer layers n or the width of the tunneling barrier is varied. In Fig. 6 the variation of $\Delta E(C,C_0;n)$ corresponding to $(\mathbf{z},\mathbf{x},\mathbf{x})$ and $(\mathbf{z},-\mathbf{z},\mathbf{x})$ and their difference with respect to the number of Cu spacers layers, n, are shown. As is to be expected both free energies show typical oscillations with respect to n. The main conclusion to be drawn is that the free energy corresponding to $(\mathbf{z},\mathbf{x},\mathbf{x})$ has to be bigger than that for $(\mathbf{z},-\mathbf{z},\mathbf{x})$, since only then do two states exist, a stable and a metastable one: a necessary precondition for switching, as already said. Of course the actual size of the difference does depend on the number of spacer layers.

In the present system the width of the tunneling barrier is only of minor importance as long as electric contact between the magnetic slabs forming the tunneling junction is prevented. Furthermore, since the maximum in the free energy (see Figs. 3 and 4) is to some extent caused by the interface of the center magnetic slab with the material forming the tunneling barrier, it seems that in terms of critical currents an optimal switching (see Fig. 4) can be achieved by varying those parameters that determine the difference in free energies shown in Fig. 6.

As in other cases[17,22] the critical current needed to switch from $(\mathbf{z},-\mathbf{z},\mathbf{z})$ (antiparallel, AP) to $(\mathbf{z},\mathbf{z},\mathbf{x})$ (parallel, P) is substantially smaller than that required to switch from P to AP. However, considering that a switching device needs to be switched back and forth, in the end only the bigger of the two critical currents counts.

Finally, it should be clear that the present investigation can only be of an academic kind, since a vacuum barrier is used instead of a realistic tunneling barrier of well-defined properties. Therefore only indirect comparisons to experiment can be made. For example, in Ref. 16 it was found that the switching time with a MgO-type barrier of unspecified width is about 5 ns, which compares reasonably well with the present value of 1.5 ns for complete switching. For the spin-valve system in Ref. 28 a switching time (at the critical current) of about 5 ns was reported. It seems therefore that between 1 and 5 ns is what presently can be achieved experimentally at room temperature. Although this is only an academic system, it seems therefore that the results shown here pinpoint reasonably well the microscopic origin of the switching properties of SV-TJ systems.

[1] J. C. Slonczewski, J. Magn. Magn. Mater. **159**, L1 (1996).
[2] X.-F. Han, A. C. C. Yu, M. Oogane, J. Murai, T. Daibou, and T. Miyazaki, Phys. Rev. B **63**, 224404 (2001).
[3] L. Lagae, R. Wirix-Speetjens, W. Eyckmans, S. Borghs, and J. De Boecka, J. Magn. Magn. Mater. **286**, 291 (2005).
[4] S. Kaka, M. R. Pufall, W. H. Rippard, T. J. Silva, S. E. Russek, J. A. Katine, and M. Carey, J. Magn. Magn. Mater. **286**, 375 (2005).
[5] G. D. Fuchs, J. A. Katine, S. I. Kiselev, D. Mauri, K. S. Wooley, D. C. Ralph, and R. A. Buhrman, Phys. Rev. Lett. **96**, 186603 (2006).
[6] F. Piéchon and A. Thiaville, Phys. Rev. B **75**, 174414 (2007).
[7] T. Devolder, C. Chappert, and K. Ito, Phys. Rev. B **75**, 224430 (2007).
[8] Y. M. Lee, J. Hayakawa, S. Ikeda, F. Matsukura, and H. Ohno, Appl. Phys. Lett. **90**, 212507 (2007).
[9] J. Barnaś, M. Gmitra, M. Misiorny, V. K. Dugaev, and H. W. Kunert, J. Non-Cryst. Solids **354**, 4181 (2008).
[10] J. C. Sankey, Y.-T. Cui, J. Z. Sun, J. C. Slonczewski, R. A. Buhrman, and D. C. Ralph, Nature Phys. **4**, 271 (2008).
[11] G. Finocchio, B. Azzerboni, G. D. Fuchs, and R. A. Buhrman, J. Appl. Phys. **101**, 063914 (2007).
[12] P. Baláž, M. Gmitra, and J. Barnaś, Phys. Rev. B **79**, 144301 (2009).
[13] H. Kikuchi, M. Sato, and K. Kobayashi, J. Appl. Phys. **87**, 6055 (2000).
[14] P. M. Bragance, J. A. Katine, N. C. Emley, D. Mauri, J. R. Childress, P. M. Rice, E. Delenia, D. C. Ralph, and R. A. Buhrman, IEEE Trans. Nanotechnol. **8**, 190 (2009).
[15] N. N. Mojumder, C. Augustine, D. E. Nikonov, and K. Roy, J. Appl. Phys. **108**, 104306 (2010).
[16] Y.-T. Cui, G. Finocchio, C. Wang, J. A. Katine, R. A. Buhrman, and D. C. Ralph, Phys. Rev. Lett. **104**, 097201 (2010).
[17] P. Weinberger, Phys. Rev. B **81**, 104417 (2010).
[18] P. Bruno and J. Wunderlich, J. Appl. Phys. **84**, 978 (2009).
[19] Xiaobing Feng, O. Bengone, M. Alouani, I. Rungger, and S. Sanvito, Phys. Rev. B **79**, 214432 (2009).
[20] Z. Li and S. Zhang, Phys. Rev. B **69**, 134416 (2004).
[21] I. N. Krivorotov, N. C. Emley, A. G. F. Garcia, J. C. Sankey, S. I. Kiselev, D. C. Ralph, and R. A. Buhrman, Phys. Rev. Lett. **93**, 166603 (2004).
[22] D. Bedau, H. Liu, J.-J. Bouzaglou, A. D. Kent, J. Z. Sun, J. A. Katine, E. E. Fullerton, and S. Mangin, Appl. Phys. Lett. **96**, 022514 (2010).

[23]P. Weinberger, Philos. Mag. **91**, 1747 (2011).
[24]J. Zabloudil, R. Hammerling, L. Szunyogh, and P. Weinberger, *Electron Scattering in Solid Matter* (Springer, Berlin, 2004).
[25]P. Weinberger, *Magnetic Anisotropies in Nanstructured Matter* (CRC Press, Boca Raton FL, 2008).
[26]The effect of using different empirical values of α in Eq. (6) for one and the same system is discussed in Ref. 27.
[27]P. Weinberger, A. Vernes, B. L. Gyorffy, and L. Szunyogh, Phys. Rev. B **70**, 094401 (2004).
[28]D. Bedau, H. Liu, J. Z. Sun, J. A. Katine, E. F. Fullerton, S. Mangin, and A. Kent, e-print arXiv:1009-5240.